SYNCHRONOUS MEASUREMENT OF THE NORMAL GROUND REACTION FORCE ON SHOE SPIKES AND FORCEPLATE

Zakir Hossain[1], Julian Grill[3], Wolfgang Grill[3], Brian MacIntosh[2]

Faculty of Kinesiology, University of Calgary, AB T2N 1N4 Canada[1,2,] ASI Analog Speed Instrument GmbH, Koenigstein im Taunus, Germany[1,3]

Monitoring balance and ground reaction forces (GRFs) during movement has obvious advantages. Sensor spikes (SS) can measure vertical GRFs while standing, walking, jogging, running, and jumping and compared with Kistler force plate. All the data from SS are derived from the time dependent voltage variations of piezo spikes, which are observed with the aid of a computer controlled transient recorder. The measurement was obtained from SS placed under the heel and forefoot. Monitoring is performed on 12 healthy subjects 29 ± 3 years of age. The force resolution is ± 0.25 N and temporal resolution is ± 0.01 ms. The contact time, take off time, impact force, active force phases of heel and forefoot have been monitored and quantified. The system is compact, battery driven and allows monitoring of the on-field GRFs during athletic and general activities.

KEY WORDS: Ground reaction force, sports dynamics, novel fall detector, on-field balance.

INTRODUCTION: Common movements in sport such as accelerating, decelerating or even simply remaining still, require ground reaction force (GRF). Measuring GRF on the sole of the shoe has potential value in competitive sports and general physical activity. In the lab, GRFs during locomotion are measured with force plates embedded in the floor. Portable sensors have also been used: in-shoe pressure sensors, accelerometers (Adrian & Cooper, 1995, Alexander, 1992, Rose & Gamble,1996), micro-electro-mechanical system (MEMS) e.g. capacitive pressure sensors (Pritchard & Mahfouz 2011). In order to attain in-field GRF data, a wearable sensor is needed. The purpose of the study was to validate force sensor in the spike of footwear, or sensor spike (SS), to measure the GRFs on contact points.

METHODS: The inexpensive piezo-electric sensors used here operate without saturation with high-pressure (www.conrad.de). They are round discs each with an impedance of 200 Ω at the resonant frequency of (6400 ± 500) Hz, a diameter of 15 mm and of 0.58 mm thick PZT layer, mounted on a 0.3 mm metal disc (Type: EPZ-20MS29). Each piezo-element had a capacitance C = 30 nF and the integrated signal gave 0.6 $mV{\bullet}N^{-1}$.

To calibrate our SS output, the SS were attached to the sensor arm of the material testing system (MTS) and compressive step loads: 0 to 0.6, 0.8, and 1kN with 2s of hold were applied (Figure 1). A piece of foam-backed artificial turf (Nexxfield©) was put below the SS. Force data of MTS and SS were recorded synchronously and compared.

To demonstrate versatility while validating the SS, we performed synchronous monitoring of vertical ground reaction force (vGRF) on SS and artificial turf covered Kistler force plate (KFP) for an athlete with a body mass of 81 kg and height 1.9 m. The athlete performed five consecutive actions for each event. Two of the ten spikes of a left cricket shoe were replaced by the SS. One underneath the posterior lateral side of the heel and the other was under the big toe, named Heel Spike (HS) and Forefoot Spike (FS). SS and KFP data were recorded synchronously for: standing, walking, running and jumping.

For the live athletic activity monitoring: twelve healthy athletes (29 ± 3) years of age, body mass (58 ± 5) kg and a BMI of 20 ± 3 were selected. Athletes wore the same pair of shoes (GM cricket shoe®, Size: UK-11, 10 spikes). The monitored movements were practiced by the athletes several times. Data were recorded first for the individual body weight, distributed to the left leg, and then for walking, jogging, running and jumping. For standing: subjects were instructed to step onto the KFP, transfer the body weight to that foot, and then quickly get back to the initial standing foot. Inflection points in the graphs are determined by local magnification and by placing the cursor on the points of interests.

RESULTS: Comparing MTS and SS: Force data from MTS and custom built SS are shown in figure1 (right). The force values observed with MTS (grey) and SS (black) for compressive step loads with 2s of hold are presented in Figure 1 and summarized in Table 1.

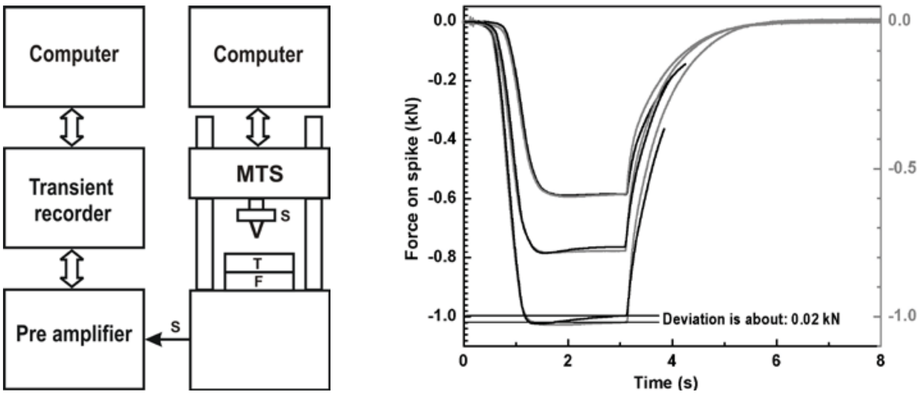

Figure 1: Schematic diagram of the data acquisition procedure (left) for measuring the reaction force on Sensor spike and Material testing system (MTS). T: Turf, F: Styrofoam layer. Right: Force for three loads. For MTS (grey) and SS (black). Force values are shown negative for compressive nature of MTS.

Table 1
The force measured at different periods with MTS and SS for programmed steps loads

Progm. Load	Peak force (kN)			Constant force (KN) applied for 2 second					
	0.6	0.8	1.0	0.6		0.8		1.0	
Time (s)	1.70	1.47	1.48	1.70	3.12	1.46	3.11	1.46	3.12
MTS	0.58	0.784	1.026	0.588	0.583	0.785	0.779	1.025	1.018
SS	0.58	0.782	1.026	0.588	0.583	0.780	0.768	0.967	0.998

The vertical GRFs detected on SS (grey) are very similar to the MTS values until peak is reached. Then during the constant load phase, there is a deviation reaching a maximum of 0.02 kN, which relates to an error of 2% for the SS in comparison to the MTS. Similar data were obtained for the 2nd SS. These data served as calibration data for the SS.

Activity monitoring: We measured force at two SS while subjects stood, walked, ran and jumped, sometimes with simultaneous recording on a Kistler force plate (KFP). For standing (Figure 2) a subject stepped onto the KFP and balanced briefly then stepped off the KFP. While force was decreasing on the heel spike, in both trials, force on the forefoot spike was increasing; then both reversed. There is a clear transfer of force from heel to forefoot and back, but this is more marked in trial 2 (right). Values for standing are shown in Table 2. Force measured on KFP at the same time didn‘t detect this transfer from back to front.

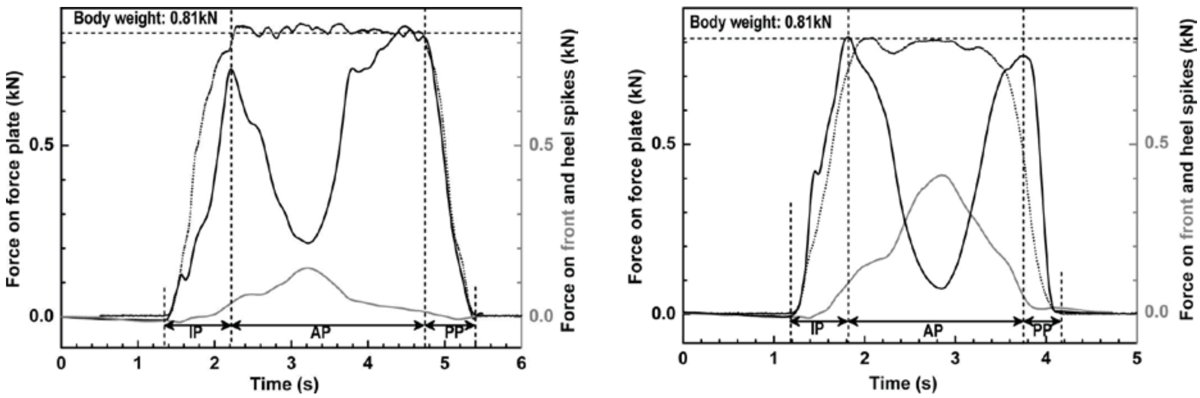

Figure 2: Synchronous measurement of vGRF’s on HS (black), FS (grey) and turf covered force plate (dotted) for standing. Trial 1 (left), and Trial 2, Different temporal phases delimited by peaks of the heel sensor are indicated (dashed) in both graphs: IP: Impact Phase, AP: Active Phase and PP: Push-off phase.

Table 2
The temporal and force quantification of different phases during transfer to one foot

Standing	IP ± 0.01 (ms)		AP ± 0.01 (ms)		PP ± 0.01(ms)	
Time	HS	KFP	HS	KFP	HS	KFP
Trial-1	855.81	854.57	2533.7	2190.75	663.05	667.45
Trial-2	638.80	790.45	1931.3	1570.25	413.05	625.95
Force	IP ± 0.25 (N)		AP ± 0.25 (N)		PP ± 0.25 (N)	
Trial-1	721.63	785.68	215.32	855.46	847.59	831.06
Trial-2	814.36	805.68	71.37	812.03	758.35	717.16

Standing force data were measured for similar athletes on synthetic floor. Sample results are given in table 3.

Table 3
The spatial quantification of different phases observed for standing

Standing	AP (N) Lowest	IP (N) Highest	AP (N/s)	PP (N)
Subject - 1	296.36 ± 0.25	580.04 ± 0.25	-110.23 ± 0.31	385.21 ± 0.25
Subject - 3	400.84 ± 0.25	582.65 ± 0.25	-101.04 ± 0.25	440.60 ± 0.25
Subject - 8	239.03 ± 0.25	603.43 ± 0.25	-160.54 ± 0.29	379.04 ± 0.25
Subject - 11	240.41 ± 0.25	545.49 ± 0.25	-171.12 ± 0.27	262.24 ± 0.25

Jumping and landing were observed synchronously on SS and KFP (see Figure 3). Results are presented in Table 4. To jump off the ground, the subject required (604 ± 0.01) ms, which is the total IP time of HS + FS. FP and LP + BP observed with FS and KFP are found to be identical.

Table 4
The temporal and force quantification of different phases observed for jumping

Jump	JO ± 0.01 (ms)			FP ± 0.01 (ms)			(LP + BP) ± 0.01 (ms)		
Time	HS	FS	KFP	HS	FS	KFP	HS	FS	KFP
Step-1	204.02	401.05	604.04	1001.4	597.10	597.12	780.15	782.26	782.24
Force	Local maximum force ± 0.25 (N)								
Step-1	1.02	2.65	2.05	0.00	0.00	0.00	5.12	-0.989	5.13

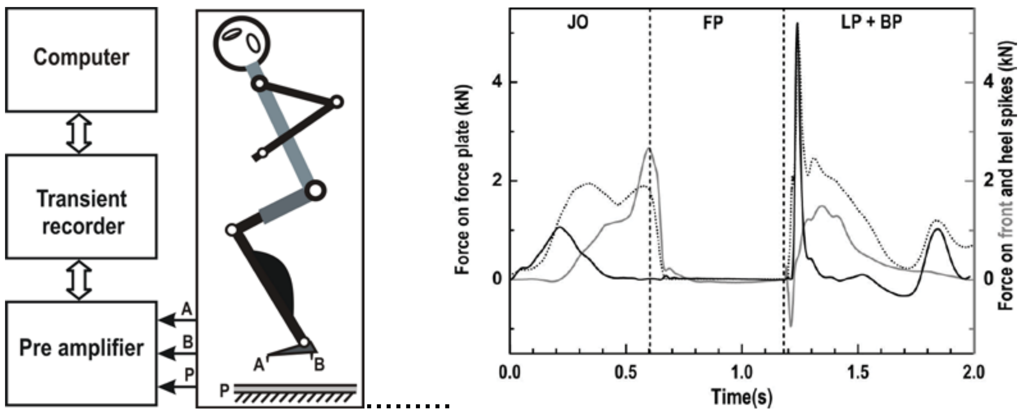

Figure 3: Schematic diagram of the data acquisition procedure (left) for on-field monitoring of the ground reaction force. A: forefoot spike sensor, B: heel spike sensor, P: force platform. Right: Graph of the data obtained for Jumping. GRFs on heel spike (black) and forefoot spike (grey). Different temporal phases are illustrated in the graph. JO: Jump off phase, FP: Flight phase, LP: Landing Phase, and BP: Balance phase.

Data for three consecutive jumps are presented in Table 5. Subject body mass was 58kg. Due to the smaller foot size, FS get little or no ground contact during jumping.

Table 5
The quantification of duration and force for three consecutive jumps

Time ± 0.01(ms)	JO	FP1	LP1	FP2	LP2	FP3	LP3
	438.20	382.15	642.70	402.201	743.25	420.20	1017.15
	Force ± 0.25 (N)						
HS	868.74	1120.92	868.74	0.00	3010.29	0.00	4415.05
FS	081.87	081.87	070.03	0.00	050.43	0.00	0.00

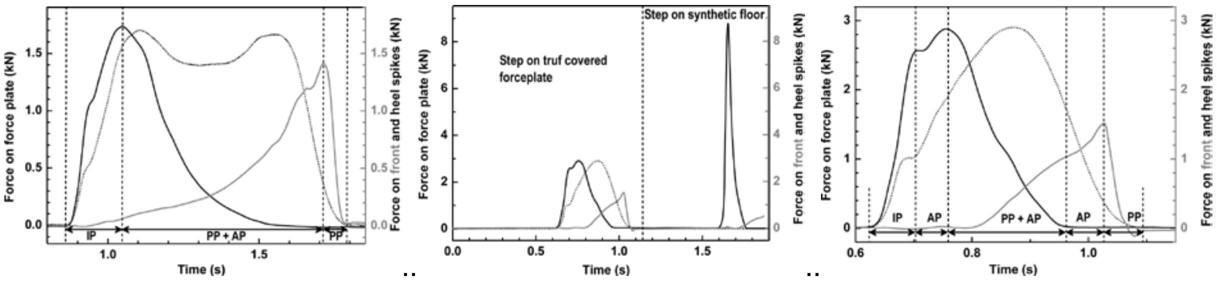

i ii iii

Figure 4. vGRFs data for walking (i) and two consecutive steps of running (ii), second step was not on of force plate but with harder synthetic surface. Step 1 is magnified in graph (iii). Temporal phases are indicated: IP: Impact Phase, AP: Active Phase and PP: Push-off phase.

Walking and running were also observed synchronously on SS and KFP (figure 4). One walking step and two running steps are shown (i and ii respectively). Quantitative results are presented in Table 6. In running, step 1 was on synthetic turf covered KFP & step-2 was outside KFP and on comparatively harder synthetic surface. Step-2 force detected on HS is much higher in magnitude (8752.61 ± 0.25) N than step-1 (2567.03± 0.25) N.

Table 6
The quantification of force and duration of phases observed for walking and running

Walking	IP ± 0.01 (ms)		AP ± 0.01 (ms)		PP ± 0.01 (ms)		
Time	HS	KFP	HS	KFP	HS	FS	KFP
Walking	200.25	203.72	98.71	487.95	664.54	69.07	277.45
Running	79.60	79.58	55.13	201.02	202.50	57.09	198.78
Force	IP ± 0.25 (N)		AP ± 0.25 (N)		PP ± 0.25 (N)		
Walking	1712.95	1701.87	1456.32	1457.46	1722.95	1413.86	1687.06
Running	2567.03	1034.03	2872.11	2602.32	2902.01	1413.86	1687.06

DISCUSSION: Clearly, movement dynamics can be quantified with SS. A unique force distribution is observed for the vGRFs shifting from HS to FS and back when weight is transferred to one foot. Similar separation of forefoot and heel distribution of force was detected while walking, running and jumping, which can be resolved with in-shoe sensors. Clarification of force difference observed between KFP and SS monitoring will require more SS placement and multidimensional SS development, which are currently underway.

CONCLUSION: The presented SS are suitable for the in-field monitoring of the GRFs on heel and forefoot of the shoe during a variety of physical activities which cannot typically be detected with conventional systems. These devices can detect stance phase or flight time. Most interestingly, differences in contact time and GRF between heel and forefoot are revealed. The sensors described in this study can be used for wireless monitoring of GRFs for human movement without impeding natural motion or restricting natural activity. Currently a lightweight assembly with a small battery operated PC is already available for monitoring of athletes. Potential uses include: steps count, energy transfer, and balance assessment.

REFERENCES:

Adrian, M. J. and Cooper, J. M. (1995). Biomechanics of Human Movement. 2nd ed. Brown and Benchmark, Madison, Wisconsin.

Alexander, R. M. (1992). The Human Machine, Natural History Museum Publications, London, 59–87.

Alexander, R. M. (1992). Exploring Biomechanics: Animals in Motion, Scientific American Library, distributed by W. H. Freeman, New York, 17–55.

Pritchard, E.R. and Mahfouz, M.R. (2011). Wireless ground reaction forces and locations across the foot using in-shoe MEMS pressure sensors. *Journal Bone Joint Surgery*, Br. 93-B:(SUPP IV) 475.

Rose, J. and Gamble, J. G. (1996). Human Walking, 2nd ed., Williams and Wilkins, Baltimore, 1–99.

Acknowledgement

Support by HPL, Kinesiology, University of Calgary is gratefully acknowledged.